The Prize Winners for 2001

E. A. Cornell (USA)
1961-
JILA and NIST
Boulder, Colorado,
USA

E. A. Cornell (USA)
1961-
JILA and NIST
Boulder, Colorado,
USA

W. Ketterle (Germany)
1957-
MIT,
Cambridge. Ma,
USA

E. A. Cornell (USA)
1961-
JILA and NIST
Boulder, Colorado,
USA

W. Ketterle (Germany)
1957-
MIT,
Cambridge. Ma,
USA

C. E. Wieman (USA)
1951-
JILA and UC,
Boulder, Colorado,
USA

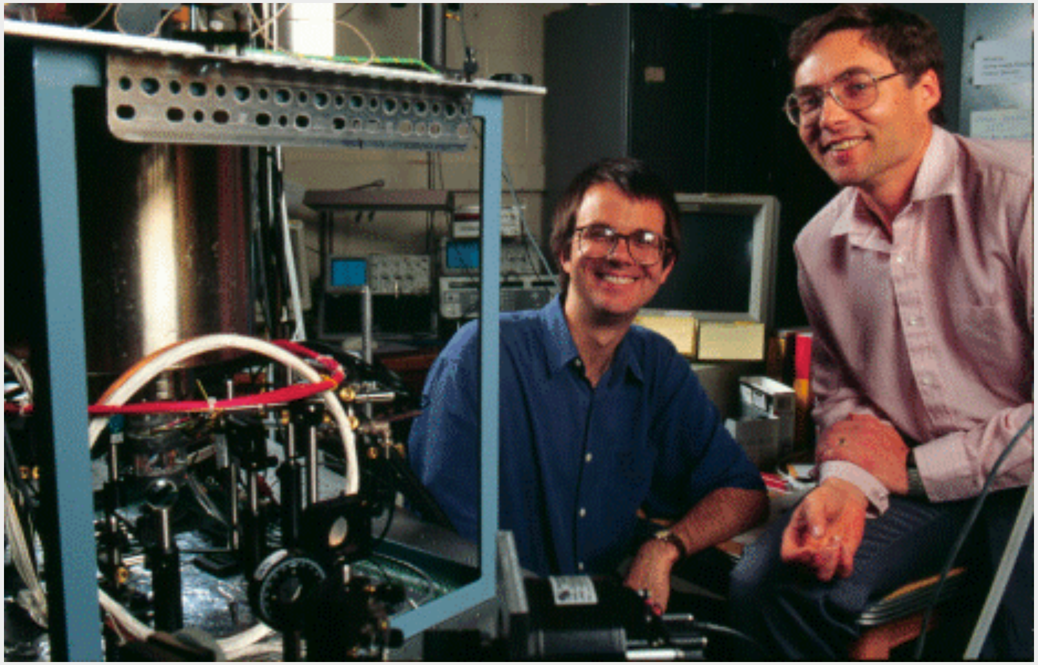

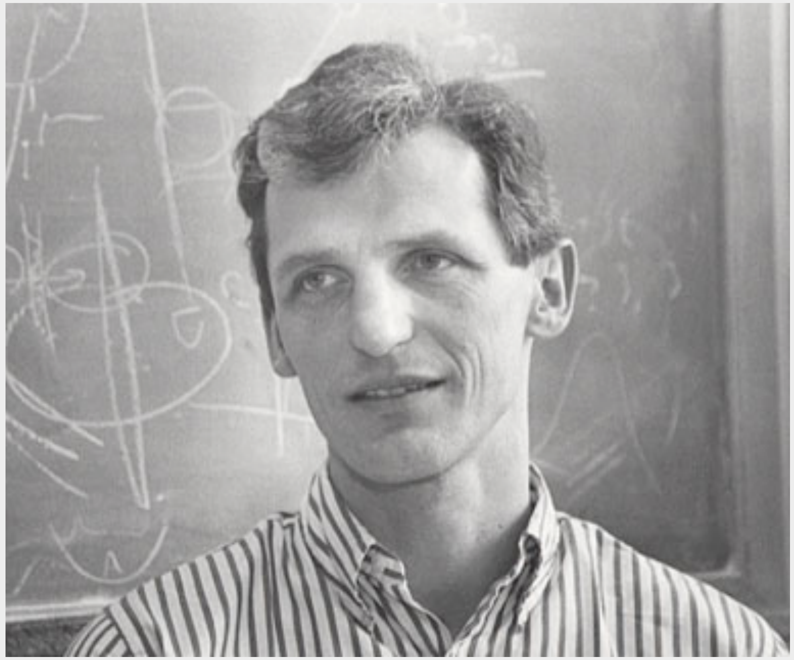

E. A. Cornell - Senior Scientist of NIST, Boulder ,Co.

W. Ketterle - John D. Mac Arthur Professor of MIT, Cambridge, Ma.

C. E. Wieman - Distinguished Professor of UC, Boulder, Co.

The Prize Winners for 2001

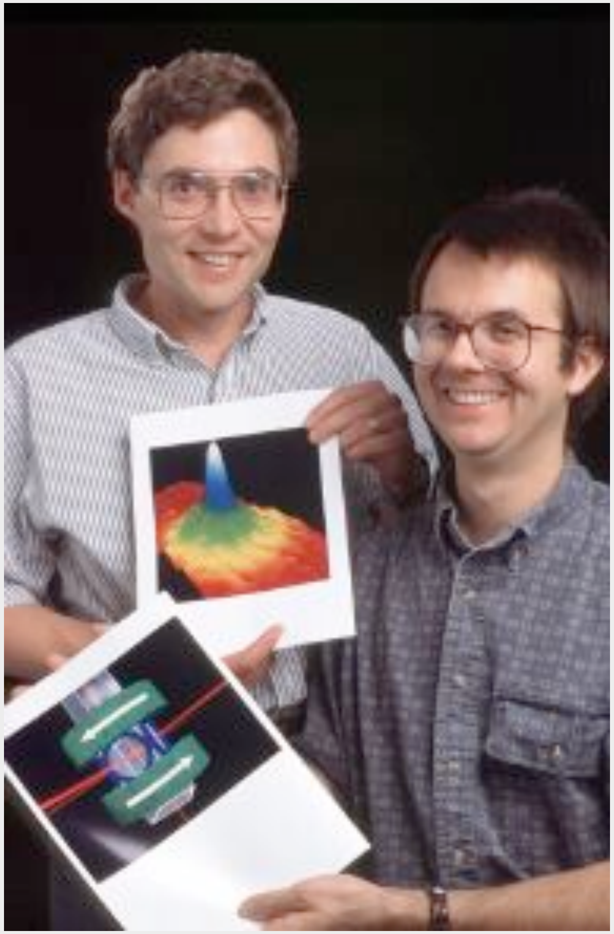

The very first condensate, Boulder, June 1995

The very first condensate, Boulder, June 1995

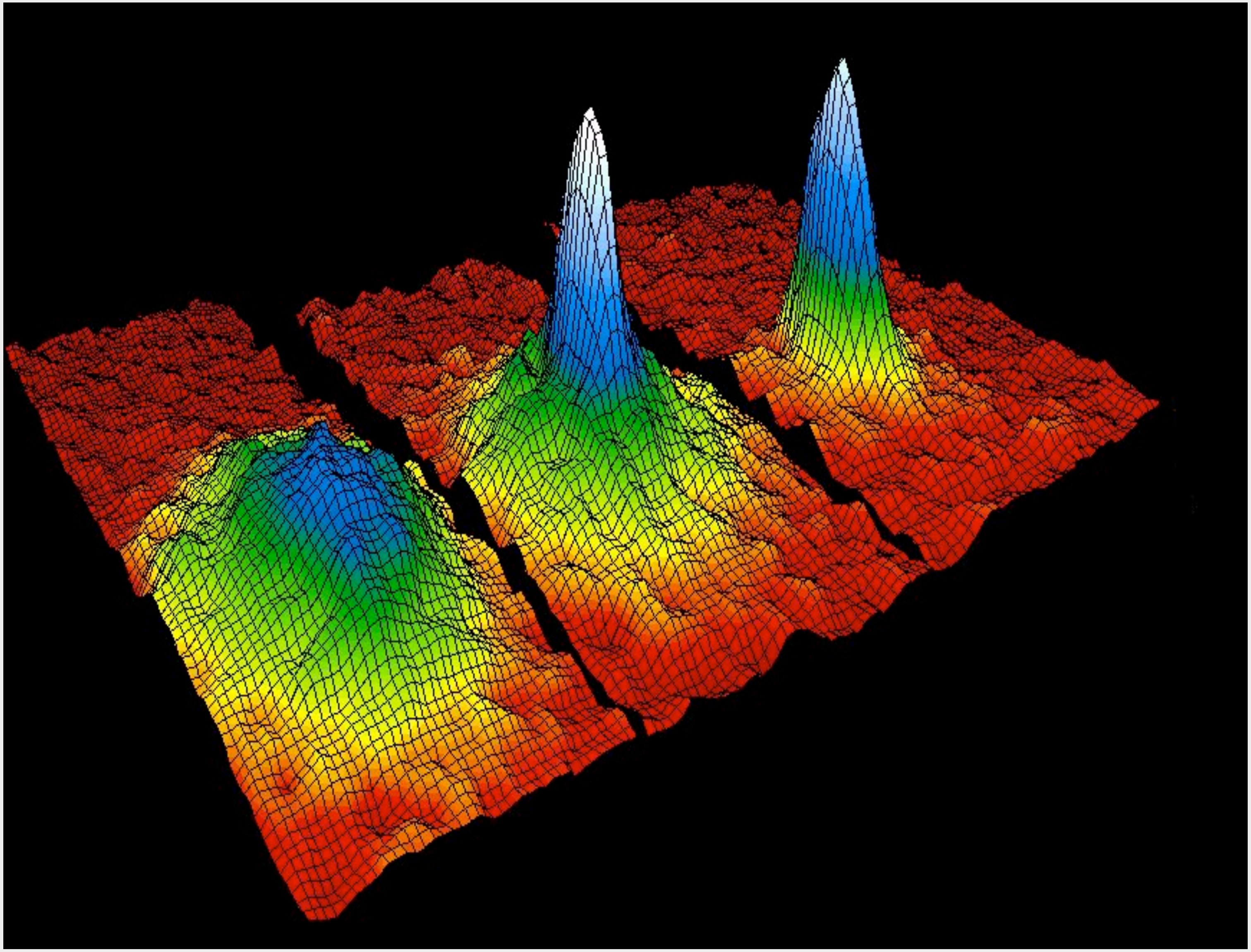

Evaporative cooling at work

Evaporative cooling at work

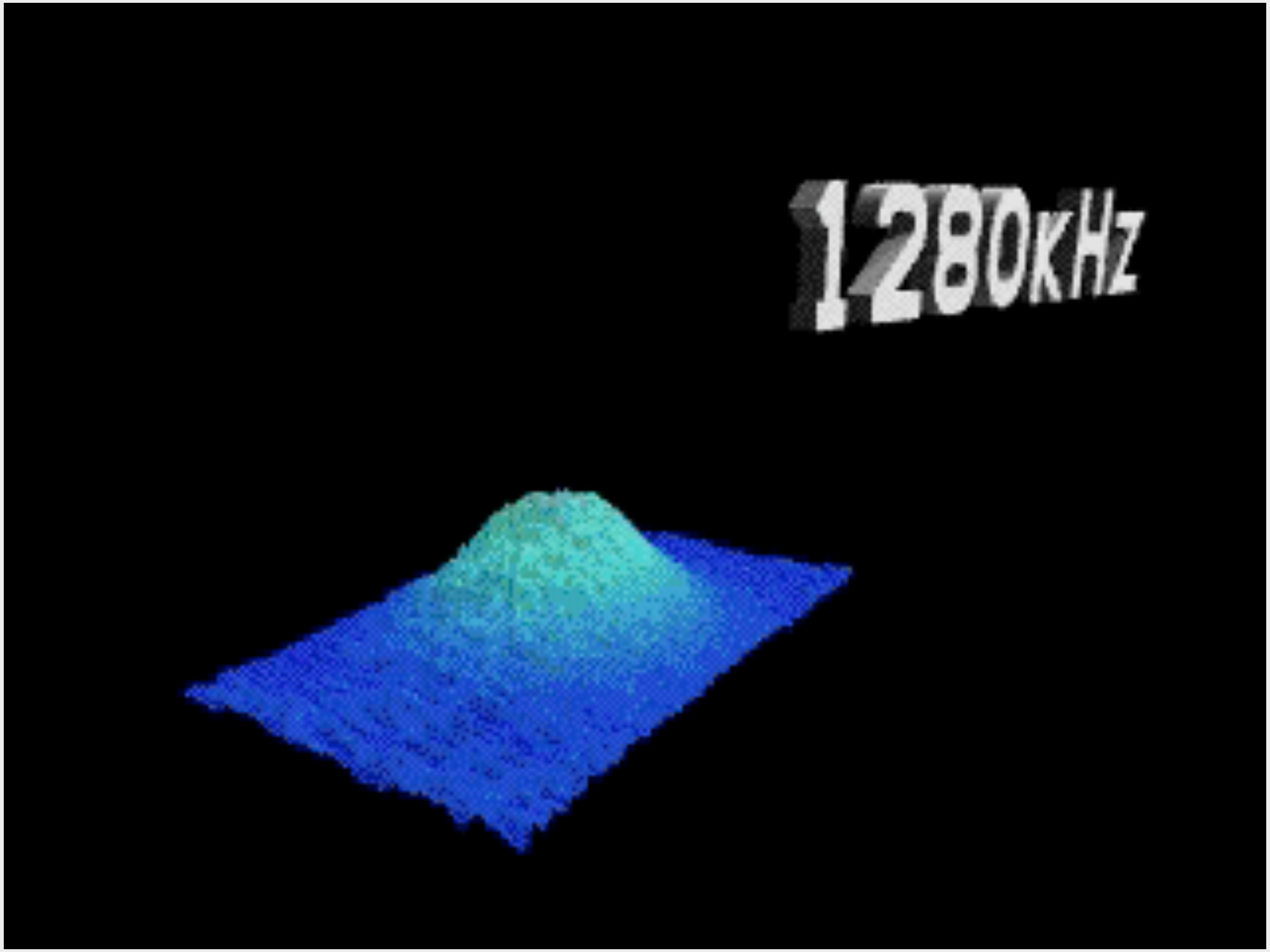

Changing aspect ratio of expanding condensate(W. Ketterle)

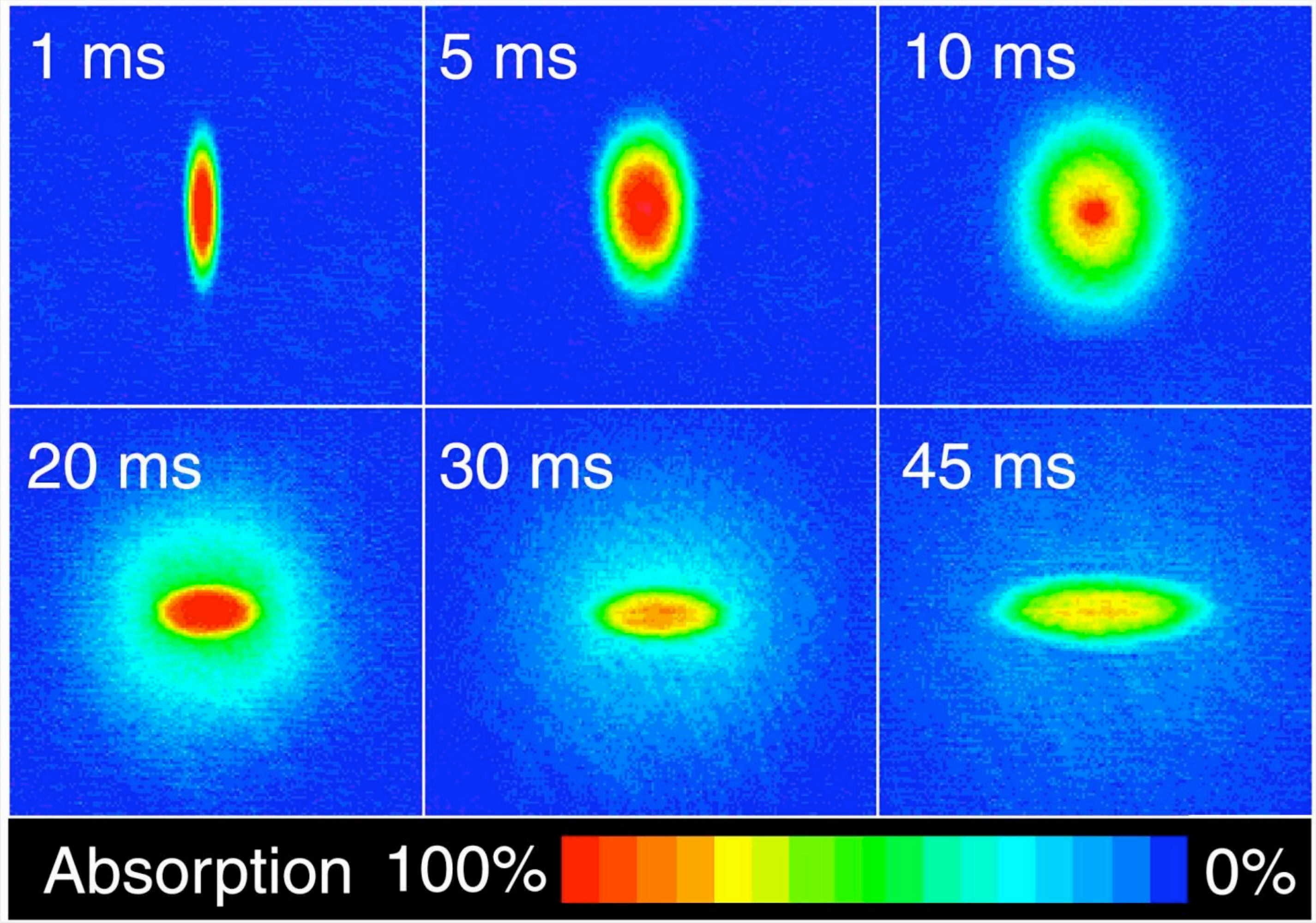

inerference of two condensates (Ketterle, Science 1997)

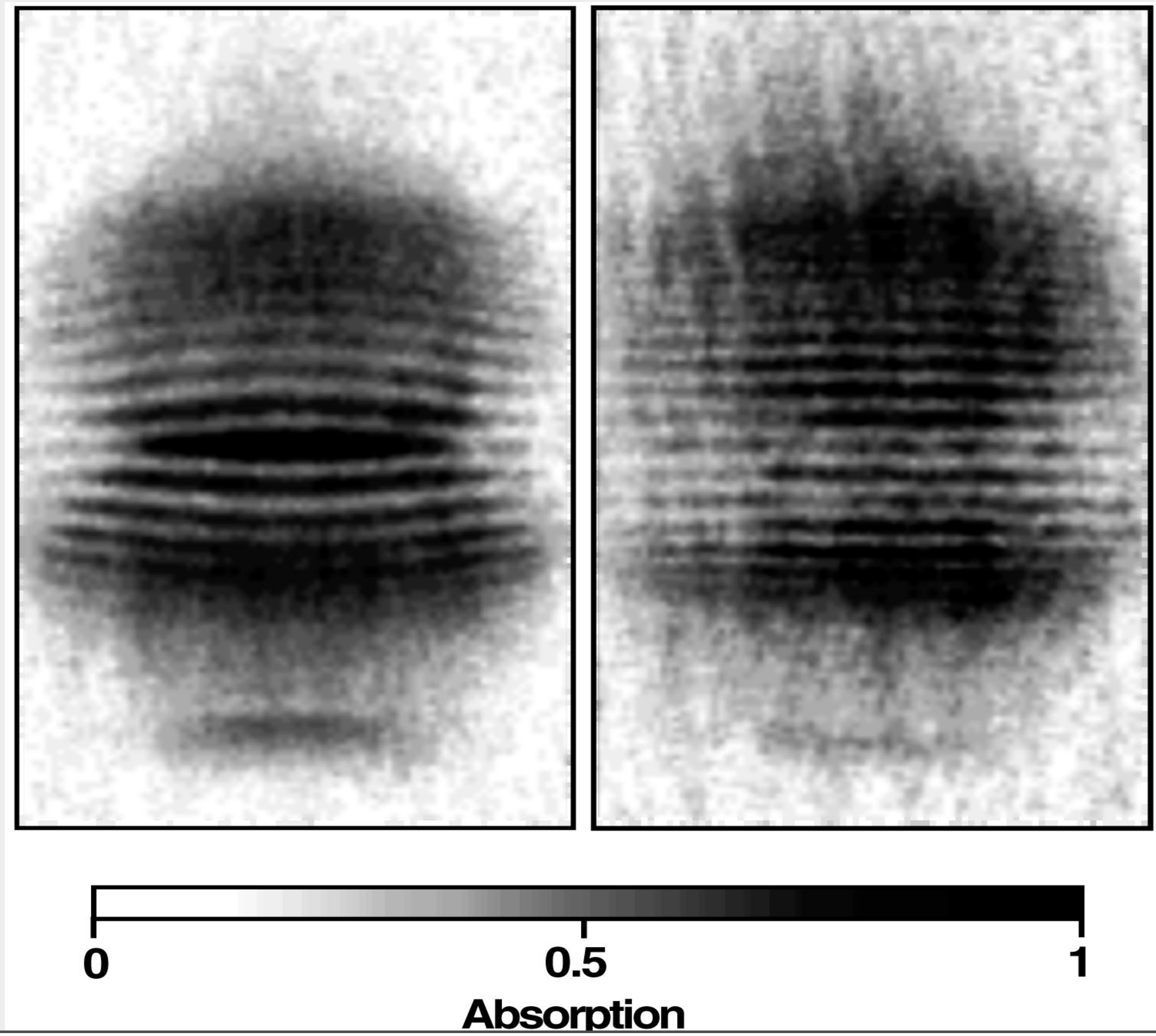

An rf output coupler: F=1

$$|BEC\rangle = (\,|m{=}{-1}\rangle)^N \;\Rightarrow$$

$$(\alpha\,|m{=}{-1}\rangle + \beta\,|m{=}0\rangle + \gamma\,|m{=}1\rangle)^N$$

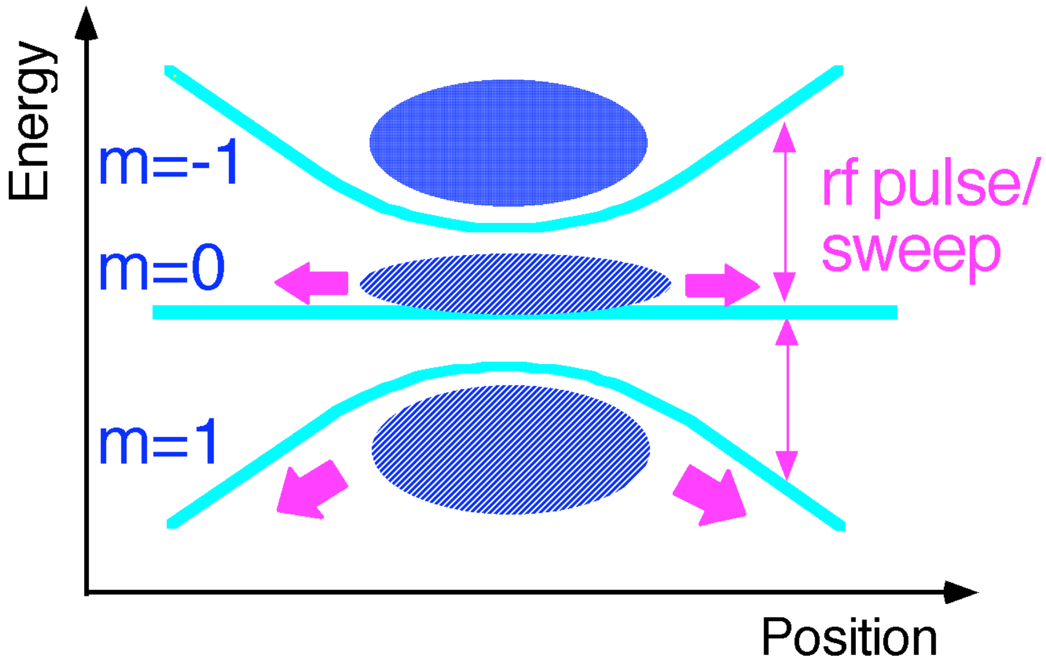

atom laser
W. Ketterle (PRL, 1997)

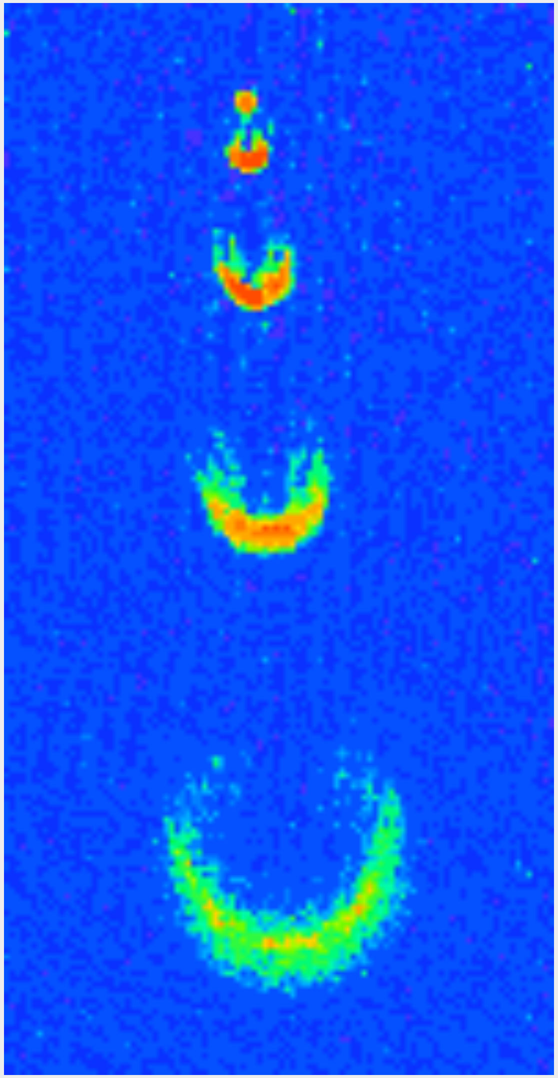

Oscillations of the condensate
(C.E. Wieman, E.A. Cornell `96)

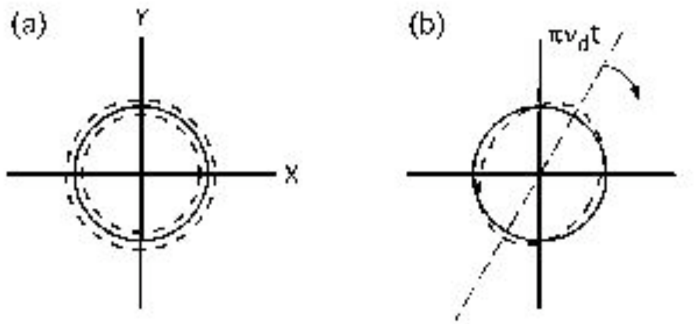

FIG. 1. In the unperturbed trap, contours of equipotential in the transverse plane are symmetric (solid line). To drive the $m = 0$ excitation (a) we apply a weak harmonic modulation with frequency ν_d to the trap radial spring constant. The $m = 2$ drive (b) breaks axial symmetry with elliptical contours which rotate at $\nu_d/2$. The amplitude of perturbation is shown exaggerated for clarity.

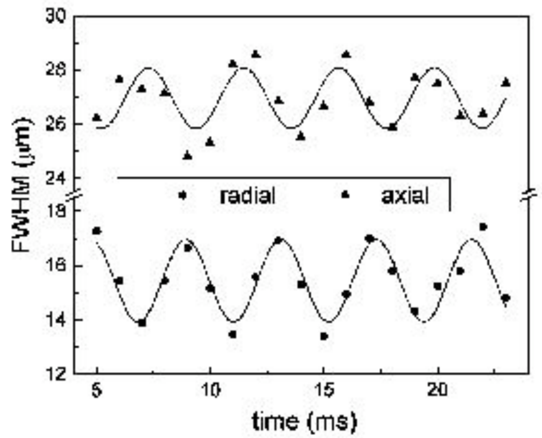

FIG. 2. We apply a weak $m = 0$ drive to an $N \approx 4500$ condensate in a 132 Hz (radial) trap. Afterward, the freely evolving response of the condensate shows radial oscillations. Also observed is a sympathetic response of the axial width, approximately 180° out of phase. The frequency of the excitation is determined from a sine wave fit to the freely oscillating cloud widths. Each data point represents a single destructive condensate measurement.

Oscillations of the condensate
(C.E. Wieman, E.A. Cornell `96)

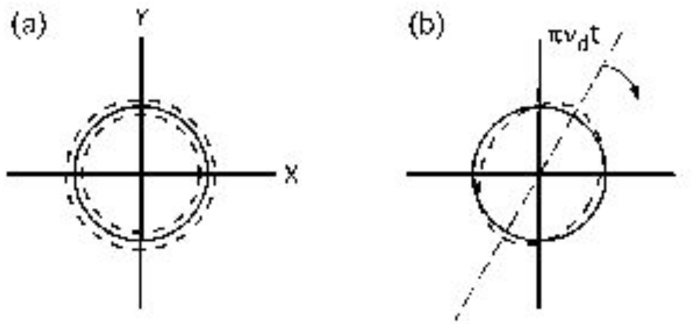

FIG. 1. In the unperturbed trap, contours of equipotential in the transverse plane are symmetric (solid line). To drive the $m = 0$ excitation (a) we apply a weak harmonic modulation with frequency ν_d to the trap radial spring constant. The $m = 2$ drive (b) breaks axial symmetry with elliptical contours which rotate at $\nu_d/2$. The amplitude of perturbation is shown exaggerated for clarity.

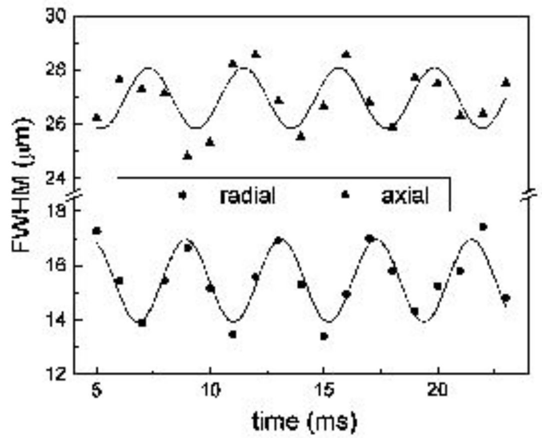

FIG. 2. We apply a weak $m = 0$ drive to an $N \approx 4500$ condensate in a 132 Hz (radial) trap. Afterward, the freely evolving response of the condensate shows radial oscillations. Also observed is a sympathetic response of the axial width, approximately 180° out of phase. The frequency of the excitation is determined from a sine wave fit to the freely oscillating cloud widths. Each data point represents a single destructive condensate measurement.

coherence of the condensate
(C.E. Wieman, E.A. Cornell `97)

loss due to three body collisions

$$\frac{dN}{dt} = -K_3 \int n^3(x,t)dt$$

local fluctuations of the thermal cloud

$$< n^3 > = 3! < n >^3$$

condensate has tiny fluctuations:

$$< n^3 > = < n >^3$$

experiment:

$$\frac{K_3^{nc}}{K_3^{c}} = 7.4\,(2.6)$$

speed of sound (W. Ketterle, 1997)

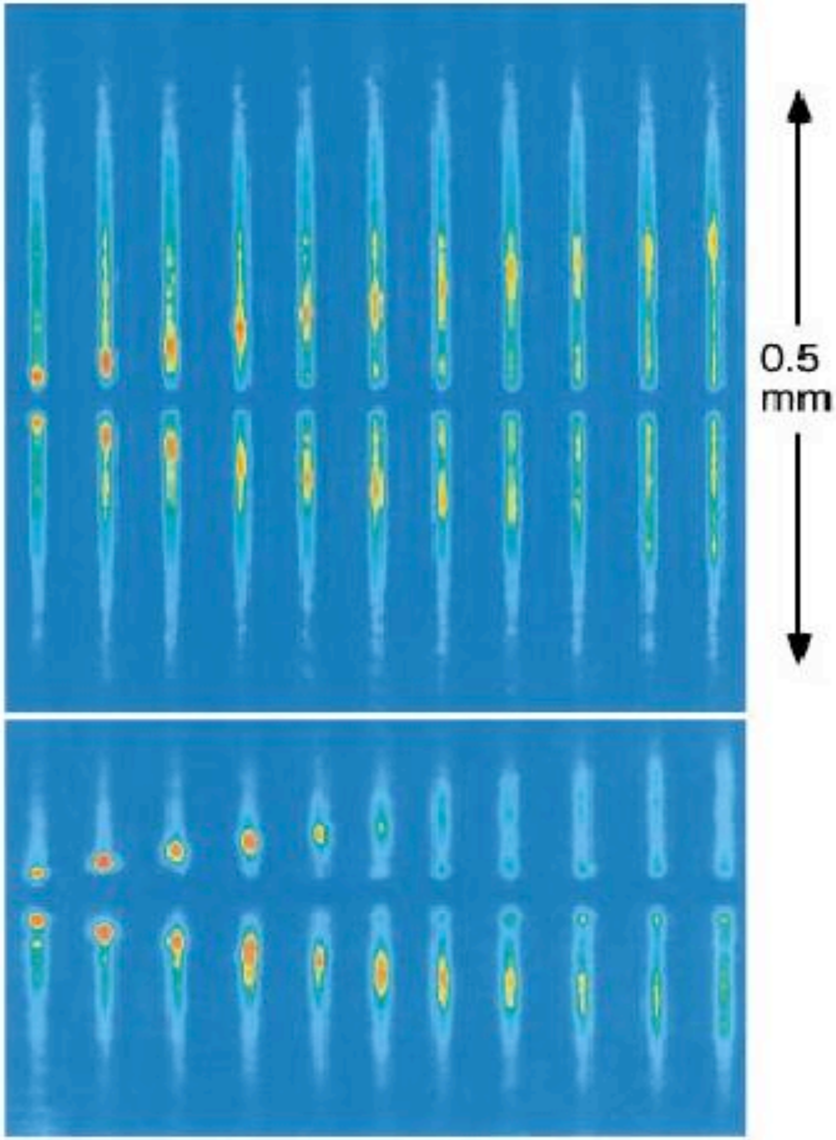

FIG. 2(color). Observation of sound propagation in a conden-

Atom laser gallery

Height:
5, 2, 0.5, 1 mm

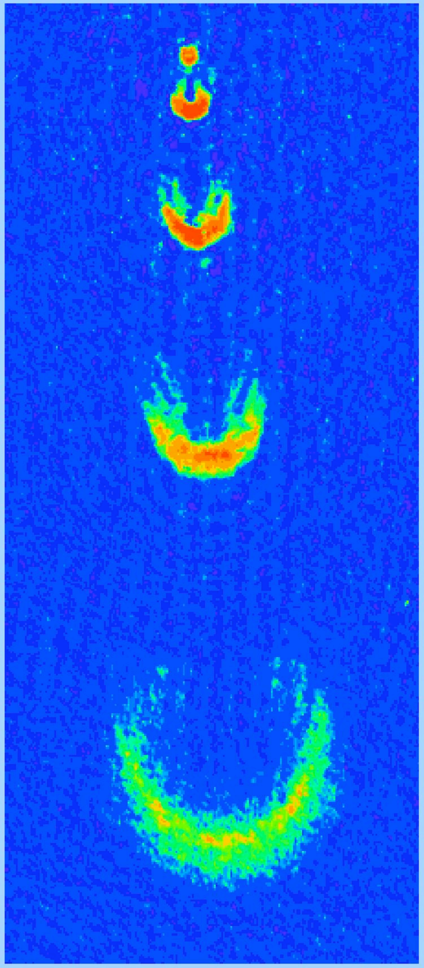

MIT '97

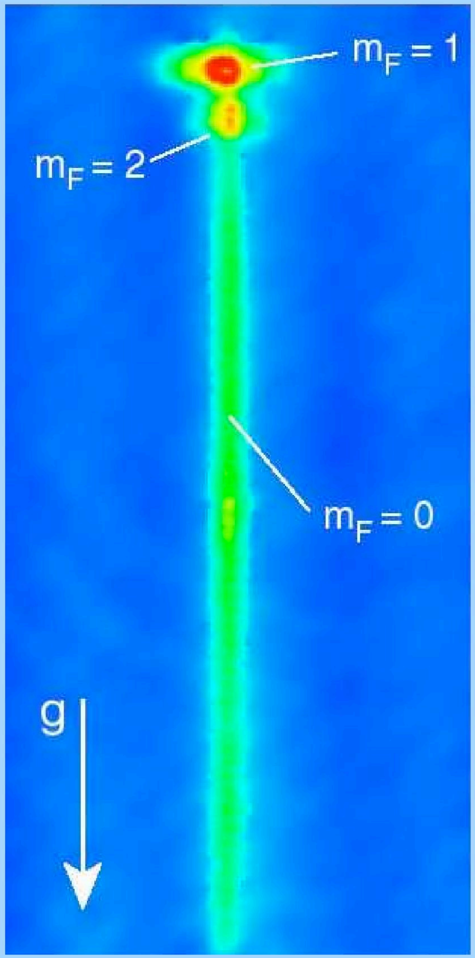

Munich '99

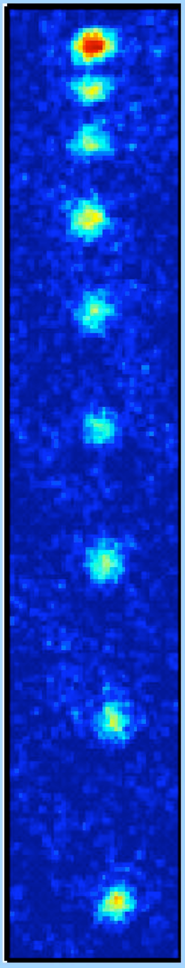

Yale '98

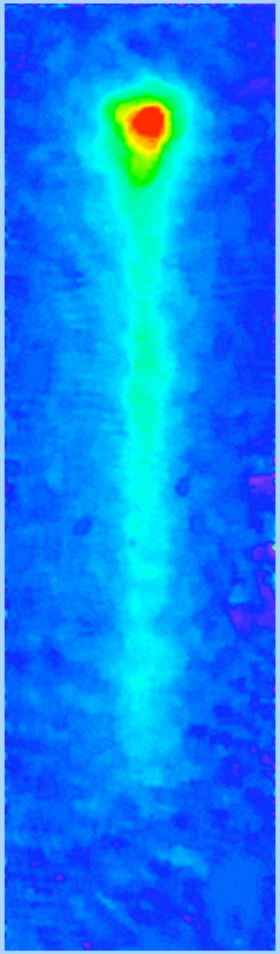

NIST '99

vortices
(W. Ketterle, Science 2001)

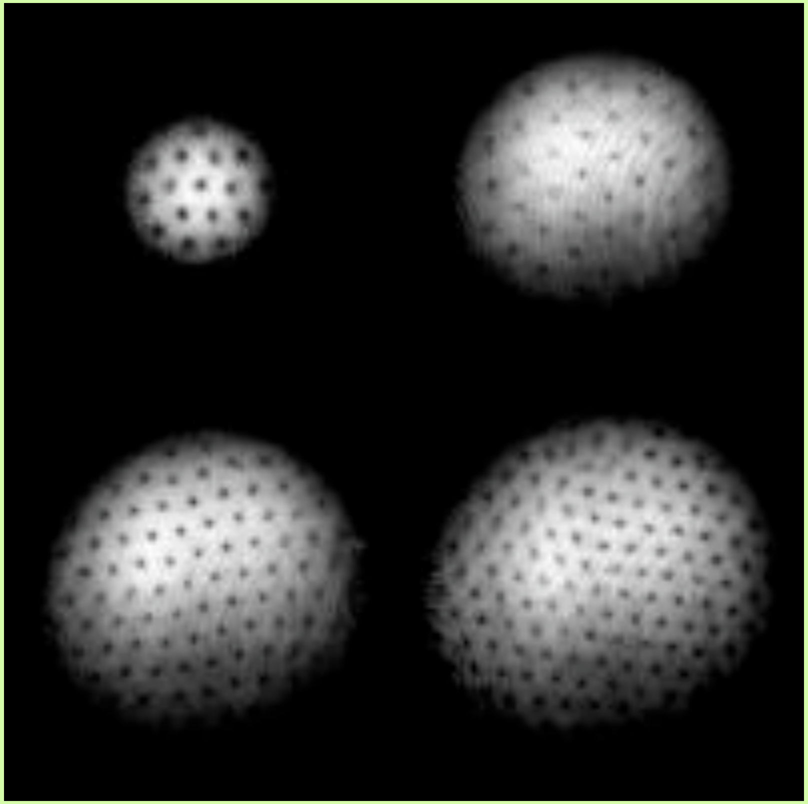

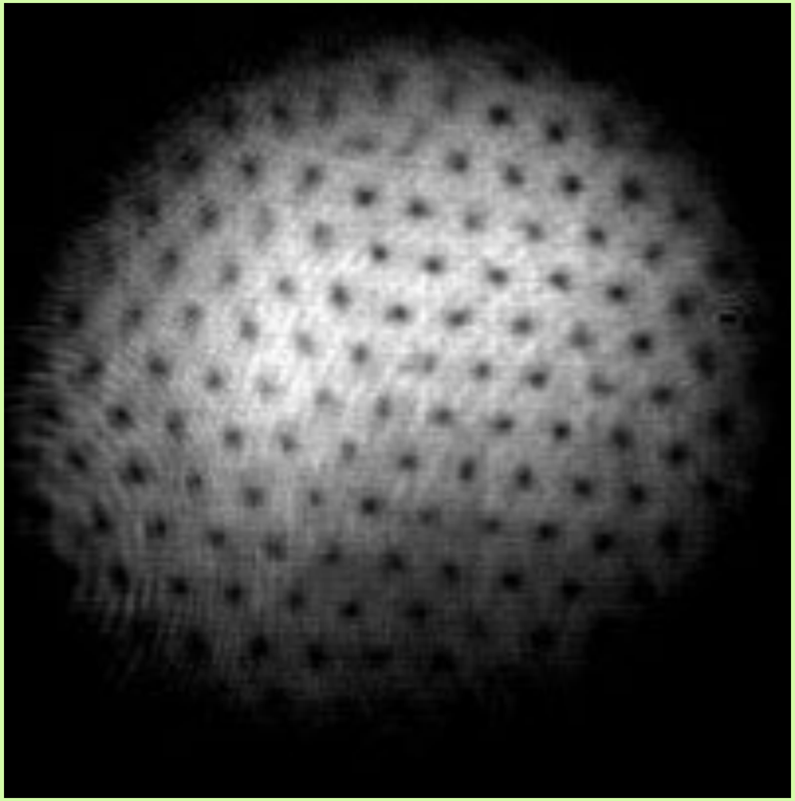

How to observe a vortex and measure its topological charge ? J. Dalibard, 2001

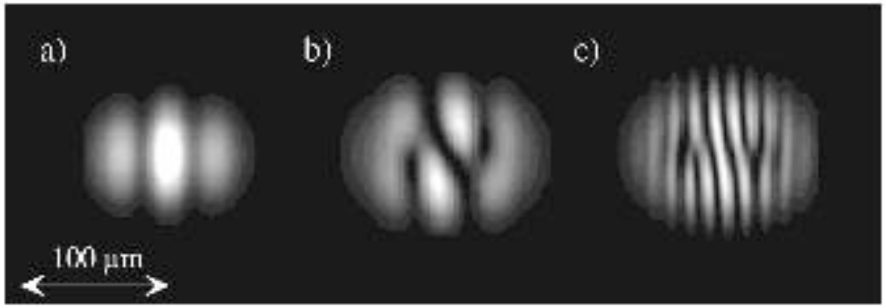

FIG. 2. Expected fringe pattern of a Bose-Einstein condensate initially splitted into two parts and undergoing a free expansion phase. Figure (a) is without a vortex and (b,c) are with a vortex. For (b), close to our experimental conditions, the fringe spacing x_s is equal to 39 μm, and it is equal to the separation of the vortex cores after expansion $|\mathbf{r}_1 - \mathbf{r}_1'|$. (c) same as (b), with a fringe spacing x_s = 13 μm $= |\mathbf{r}_1 - \mathbf{r}_1'|/3$ (this fringe spacing is too small to be detected in our experimental setup). For (b) and (c), the relative phase of the two condensates is π.

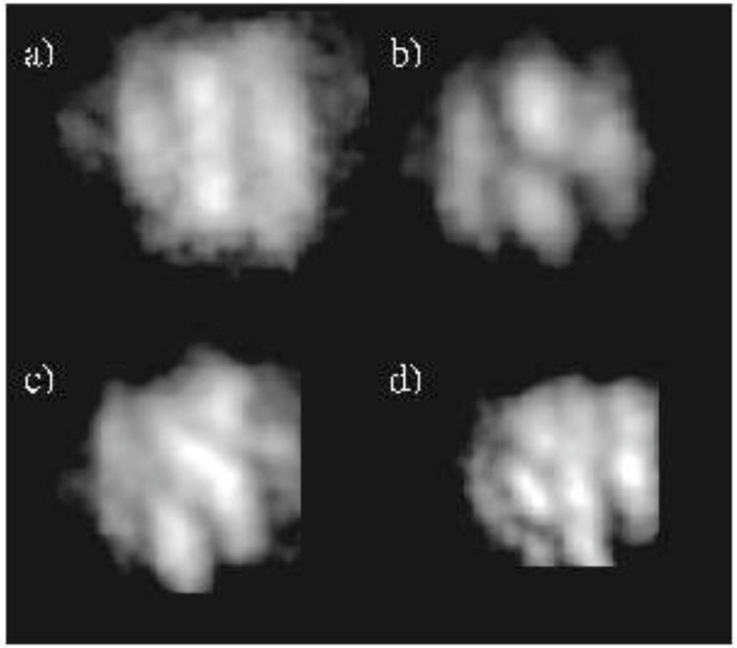

FIG. 4. Interference pattern measured in the $m=+2$ channel with no (a), one (b) and (c), and several (d) vortices. For these pictures, $\tau_1 = 0.688$ ms and $\tau_2 = 1.320$ ms. The stirring frequency was set to $\Omega = 2\pi \times 125$ Hz (a), $\Omega = 2\pi \times 130$ Hz (b-c), and $\Omega = 2\pi \times 154$ Hz (d). The patterns (b) and (c) were recorded with the same initial conditions, and the change in the interference pattern results from a change in the relative phase of the two parts of the condensate.

bouncing condensate off a laser mirror (W. Ertmer, 1999)

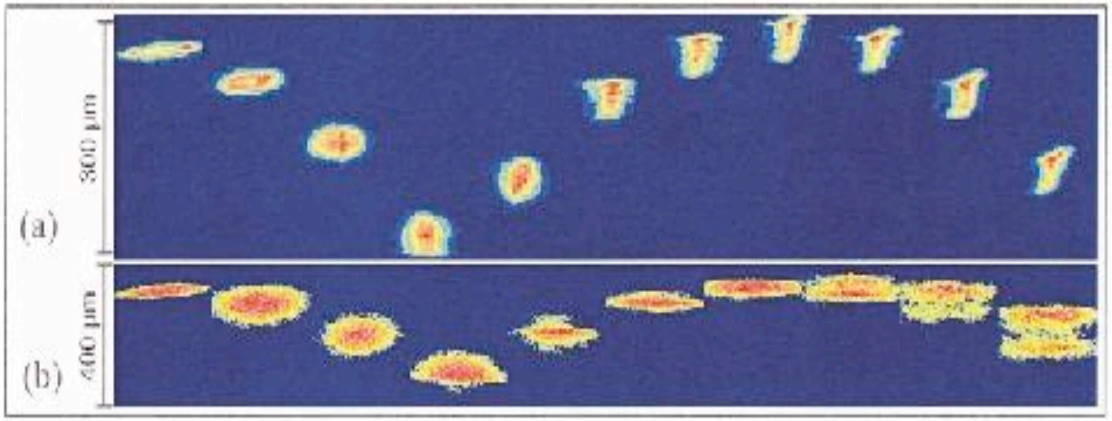

FIG. 1 (color). (a) Series of dark field images for condensates bouncing off a light sheet 270 μm below the magnetic trap. Each image was taken with a new condensate and with an additional time delay of 2 ms. The density of the condensate during the first few ms of expansion causes a phase shift in the detection light of more than 2π, which explains the stripes in the middle of the first two images. (b) A thermal cloud bouncing off a light sheet situated 230 μm below the magnetic trap splits into two parts.

3578

spinor condensates

optical dipole traps hold atoms with all orientations of spin.

contact interaction of two
F=1 atoms

$$V = V_0 P_0 + V_2 P_2 \qquad (F_1 = F_2 = 1)$$

projection operators

$$P_0 = \frac{1}{3}\left(1 - \vec{F}_1 \vec{F}_2\right)$$

$$\vec{F}_1 \cdot \vec{F}_2 = \frac{(\vec{F}_1 + \vec{F}_2)^2 - \vec{F}_1^{\,2} - \vec{F}_2^{\,2}}{2}$$

$$P_2 = \frac{1}{3}\left(2 + \vec{F}_1 \vec{F}_2\right)$$

resulting interaction operator

$$V = \frac{1}{3}\left(V_0 + 2V_2\right) + \frac{1}{3}\left(V_2 - V_0\right)\vec{F}_1 \vec{F}_2$$

contact interaction continued

$$V_0 = \frac{4\pi\hbar^2 a_0}{m}\delta(\vec{r}_1 - \vec{r}_2)$$

$$V_2 = \frac{4\pi\hbar^2 a_2}{m}\delta(\vec{r}_1 - \vec{r}_2)$$

$$\left[V, L_{1z} + L_{2z}\right] = 0$$

$$\left[V, F_{1z} + F_{2z}\right] = 0$$

$$\hat{H} = \int d^3r \left(\hat{\psi}_i^+ H_0 \hat{\psi}_i + \tfrac{1}{2} c_0\, \hat{\psi}_j^+ \hat{\psi}_i^+\, \hat{\psi}_i \hat{\psi}_j + \tfrac{1}{2} c_2\, \hat{\psi}_k^+ \hat{\psi}_i^+ \vec{F}_{ij} \vec{F}_{kl}\, \hat{\psi}_j \hat{\psi}_l\right)$$

$$c_0 = \frac{4\pi\hbar^2}{m}\frac{1}{3}(a_0 + 2a_2)$$

$$c_2 = \frac{4\pi\hbar^2}{m}\frac{1}{3}(a_2 - a_0)$$

conventional choice of spin matrices:

$$F_x = \frac{1}{\sqrt{2}}\begin{bmatrix} 0 & 1 & 0 \\ 1 & 0 & 1 \\ 0 & 1 & 0 \end{bmatrix} \quad F_y = \frac{1}{\sqrt{2}}\begin{bmatrix} 0 & -i & 0 \\ i & 0 & -i \\ 0 & i & 0 \end{bmatrix} \quad F_z = \begin{bmatrix} 1 & 0 & 0 \\ 0 & 0 & 0 \\ 0 & 0 & -1 \end{bmatrix}$$

For ^{87}Rb $c_2<0$ and the ground state is ferromagnetic

assuming a single, universal, spatial mode:

$$\psi_i(\vec{r}) = \sqrt{n(\vec{r})}\,\xi_i(\vec{r})$$

the energy functional takes a form

$$E = \int d^3r \left(\frac{\hbar^2}{2m}(\nabla\sqrt{n})^2 + \frac{\hbar^2}{2m}|\nabla\xi|^2 n + V(\vec{r})n + \frac{n^2}{2}\left(c_0 + c_2\left\langle\vec{F}\right\rangle^2\right)\right)$$

$$\left\langle\vec{F}\right\rangle = \xi_i \vec{F}_{ij} \xi_j$$

and has a minimum for **the maximal value of the spin**

(more complicated *F*=2 state of rubidium is antiferromagnetic)

20

minimizing we get:

$$\xi = U \begin{bmatrix} 1/2 \\ 1/\sqrt{2} \\ 1/2 \end{bmatrix}$$

$$P = [1/4, 1/2, 1/4]$$

averaging over all angles:

$$< P > = [1/3, 1/3, 1/3]$$

Domeny magnetyczne w kondensacie rubidowym o F=1 (D. Stamper-Kurn - Berkeley 2007)